A family of stable iron(I) σ-alkynyl complexes. Synthesis, characterization, structure, and electron-transfer chemistry

ARTICLE *in* JOURNAL OF THE AMERICAN CHEMICAL SOCIETY · APRIL 1993

Impact Factor: 12.11 · DOI: 10.1021/ja00060a022

A Family of Stable Iron(I) σ-Alkynyl Complexes. Synthesis, Characterization, Structure, and Electron-Transfer Chemistry

Claudio Bianchini,*,† Franco Laschi,§ Dante Masi,† Francesca M. Ottaviani,‡ Antonio Pastor,† Maurizio Peruzzini,*,† Piero Zanello,*,§ and Fabrizio Zanobini†

Contribution from the Istituto per lo Studio della Stereochimica ed Energetica dei Composti di Coordinazione, CNR, Via J. Nardi 39, 50132 Florence, Italy, Dipartimento di Chimica, Università di Siena, Via Pian dei Mantellini 44, 53100 Siena, Italy, and Dipartimento di Chimica, Università di Firenze, Via G. Capponi 9, 50100 Florence, Italy

Received February 5, 1992

Abstract: Fe(II) and Fe(I) σ-alkynyl complexes of the general formula $[(PP_3)Fe(C{\equiv}CR)]^{n+}$ (n = 1, 0) have been synthesized as BPh_4^- salts or neutral molecules and characterized by chemical, spectroscopic, X-ray, and electrochemical techniques [R = Ph, $SiMe_3$, n-C_3H_7, n-C_5H_{11}, CMe_3; PP_3 = $P(CH_2CH_2PPh_2)_3$]. All of the compounds undergo electron-transfer reactions that encompass Fe(0), Fe(I), Fe(II), and Fe(III) oxidation states of the metal. X-ray crystal structures of the 16- and 17-electron complexes $[(PP_3)Fe(C{\equiv}CPh)]BPh_4{\cdot}C_4H_8O$ and $[(PP_3)Fe(C{\equiv}CPh)]$ have been determined. The Fe(II) compound crystallizes in the space group $P2_1/c$, and the cation assumes an almost regular trigonal-bipyramidal structure with the alkynyl ligand trans to the bridgehead phosphorus atom of PP_3 (P_4–Fe–C_7 bond angle = 177.2(6)°). The Fe(I) compound crystallizes in the space group $P2_1/n$ and assumes a strongly distorted trigonal-bipyramidal structure with the P_4–Fe–C_7 bond angle of 170.3(3)° and equatorial bond angles of 143.9(1)°, 102.4(1)°, and 111.1(1)°. A decrease in the Fe–P bond distances on going from Fe(II) to Fe(I) is interpreted in terms of significant metal → phosphorus π-back-bonding. In contrast, from a perusal of IR, structural, and electrochemical data, no significant dπ (metal) → π* (alkynyl) interaction occurs. All compounds are paramagnetic and have been characterized by X-band ESR spectroscopy (powder, frozen solution, fluid solution). The powder and frozen solution spectra of the Fe(I) alkynyls are interpreted in terms of $S = {}^1/_2$ and a rhombic **g** tensor. The fluid solution spectra show that the compounds exist in tetrahydrofuran solution as two isomeric forms exhibiting distorted trigonal-bipyramidal structures in a ratio that depends on the temperature. The ESR spectra of the Fe(II) derivatives (powder and frozen solution) display unresolved line shape consistent with a S = 1 Hamiltonian with noticeable zero-field splitting effects at room temperature.

Introduction

The oxidation state +1 in iron coordination chemistry is interesting for its rarity.[1] In fact, though isoelectronic with ubiquitous Co(II) complexes, d^7 iron(I) derivatives are generally unstable with respect to the disproportionation to iron(0) and iron(II) species. Iron(I) organometallic compounds are even more rare, being essentially limited to phosphine and carbonyl complexes with unsaturated cyclic hydrocarbons (η^5-C_5H_5,[2,3] η^4-C_4Ph_4,[4] η^6-C_6R_6,[5] η^3-C_8H_{13}[6]). To the best of our knowledge, no stable iron(I) compound with a σ-hydrocarbyl has ever been reported.

In this paper, we describe the synthesis, the X-band ESR characterization, and the electrochemical behavior of a family of d^7 low-spin σ-alkynyl Fe(I) complexes of the general formula $[(PP_3)Fe(C{\equiv}CR)]$ (PP_3 = $P(CH_2CH_2PPh_2)_3$; R = Ph, $SiMe_3$, n-C_3H_7, n-C_5H_{11}, CMe_3).

Comparisons will be made with the d^6 paramagnetic iron(II) congeners $[(PP_3)Fe(C{\equiv}CR)]BPh_4$ in order to establish to what extent the addition/removal of one electron to the "$(PP_3)Fe(C{\equiv}CR)$" moiety may affect the chemicophysical properties of the complexes. In this respect, valuable information has been obtained from a comparison of the X-ray structures of the redox couple formed by the two phenylethynyl complexes $[(PP_3)Fe(C{\equiv}CPh)]$ and $[(PP_3)Fe(C{\equiv}CPh)]^+$.

It is expected that the large scale preparation of the title compounds and of their Fe(II) analogs will open the way to a systematic study of the chemistry of paramagnetic σ-alkynyl metal complexes of which only a few examples of ionic species are known.[7]

Experimental Section

General Data. Tetrahydrofuran (THF), dichloromethane, and n-hexane were purified by distillation over $LiAlH_4$, P_2O_5, and Na, respectively, just prior to use. 1-Alkynes were purchased from either Fluka or Aldrich and checked by ^1H NMR spectroscopy. When necessary, they were distilled prior to use. All the other reagents and chemicals were reagent grade and, unless otherwise stated, were used as received by commercial suppliers. All reactions and manipulations were routinely performed under a dry argon or nitrogen atmosphere using Schlenk tube techniques. The solid complexes were collected on sintered-glass frits and washed with ethanol and petroleum ether (bp 40–70 °C) before being dried in a stream of nitrogen. Literature methods were used for the preparation of $[(PP_3)Fe(C{\equiv}CPh)]BPh_4$ (**1**),[8a] $[(PP_3)Fe(C{\equiv}CSiMe_3)]BPh_4$ (**2**),[8a] $[(PP_3)Fe(H)(H_2)]BPh_4$ (**3**),[9] $[(PP_3)Fe(H)(N_2)]BPh_4$ (**4**),[10]

† CNR Florence.
§ University of Siena.
‡ University of Florence.

(1) (a) Hawker, P. N.; Twigg, M. V. *Comprehensive Coordination Chemistry*; Wilkinson, G., Ed.; Pergamon Press: New York, 1987; Vol. IV, p 1179. (b) Cotton, F. A.; Wilkinson, G. *Advanced Inorganic Chemistry*, 5th ed.; Wiley Interscience: New York, 1988.

(2) Eisch, J. J.; King, R. B. In *Organometallic Synthesis*; Academic Press: New York, 1965; Vol. I, p 114.

(3) Hamou, J. R.; Astruc, D.; Michaud, P. *J. Am. Chem. Soc.* **1981**, *103*, 758.

(4) Orpen, A. G.; Connelly, N. G.; Whiteley, M. W.; Woodward, P. *J. Chem. Soc., Dalton Trans.* **1989**, 1751.

(5) Astruc, D.; Mandon, D.; Madonik, A.; Michaud, P.; Ardoin, N.; Varret, F. *Organometallics* **1990**, *9*, 2155.

(6) Harlow, R. L.; McKinney, R. J.; Ittel, S. D. *J. Am. Chem. Soc.* **1979**, *101*, 7496.

(7) (a) Nast, R. *Coord. Chem. Rev.* **1982**, *47*, 89. (b) Bianchini, C.; Innocenti, P.; Meli, A.; Peruzzini, M.; Zanobini, F.; Zanello, P. *Organometallics* **1990**, *9*, 2514. (c) Bianchini, C.; Meli, A.; Peruzzini, M.; Vacca, A.; Laschi, F.; Zanello, P.; Ottaviani, M. F. *Organometallics* **1990**, *9*, 360.

(8) (a) Bianchini, C.; Meli, A.; Peruzzini, M.; Frediani, P.; Bohanna, C.; Esteruelas, M. A.; Oro, L. A. *Organometallics* **1992**, *11*, 138. (b) Bianchini, C.; Meli, A.; Peruzzini, M.; Vizza, F.; Zanobini, F.; Frediani, P. *Organometallics* **1989**, *8*, 2080.

(9) (a) Bianchini, C.; Peruzzini, M.; Zanobini, F. *J. Organomet. Chem.* **1988**, *354*, C19. (b) Bianchini, C.; Peruzzini, M.; Polo, A.; Vacca, A.; Zanobini, F. *Gazz. Chim. Ital.* **1991**, *121*, 543.

0002-7863/93/1515-2723$04.00/0

and $[(C_5H_5)_2Fe]PF_6$.[11] $[(C_5H_5)_2Co]$ was purchased from Strem Chemicals and used without further purification.

Deuterated chloroform for NMR measurements (Janssen) was dried over molecular sieves. Proton NMR spectra were recorded on VARIAN VXR 300 and BRUKER AC 200P instruments operating at 299.94 and 200.13 MHz, respectively. Peak positions are relative to tetramethylsilane as an external reference. Infrared spectra were recorded on a Perkin-Elmer 1600 Series FTIR spectrophotometer using samples mulled in Nujol between KBr plates. Conductivities were measured with an ORION Model 990101 conductance cell connected to a Model 101 conductivity meter. The conductivity data were obtained at sample concentrations of ca. 1×10^{-3} M in nitroethane solutions at room temperature (22 °C). Magnetic susceptibilities of solid samples were measured on a Faraday balance at room temperature.

Cyclic voltammetry was performed in a three-electrode cell having either a platinum or mercury (mercury coated gold sphere) working electrode surrounded by a platinum-spiral counter electrode and the aqueous saturated calomel reference electrode (SCE) mounted with a Luggin capillary. Either a BAS 100A electrochemical analyzer or a multipurpose Amel instrument (a Model 566 analog function generator and a Model 552 potentiostat) was used as the polarizing unit. Controlled potential coulometric tests were performed in a H-shaped cell with anodic and cathodic compartments separated by a sintered-glass disk. The working macroelectrode was a platinum gauze; a mercury pool was used as the counter electrode. The Amel potentiostat was connected to an Amel Model 558 integrator. Tests at low temperature were carried out by using an Ag/AgCl reference electrode. All the potentials values are referred to the SCE. ESR measurements were taken on a Bruker ER 200-SRDD spectrometer operating at X-band (ω_o = 9.78 GHz). The operational microwave frequency (BRUKER Microwawe bridge ER 041 MR) was tested with an XL microwawe frequency counter 3120 and the external magnetic field H_0 was calibrated by using a DPPH powder sample (g_{DPPH} = 2.0036). The temperature was controlled with a Bruker ER 4111 VT device with an accuracy of ±1 °C. The samples were placed in quartz flat cells positioned in the resonance cavity. Computer simulation of the ESR spectra was carried out by using the SIM14 A program[12] appropriately modified so as to include in the calculations, for an orthorombic g value, up to four different nuclei with orthorombic A values.

Synthesis of the Iron(II) Alkynyls $[(PP_3)Fe(C{\equiv}CR)]BPh_4$ (R = *n*-C_3H_7, 5; *n*-C_5H_{11}, 6; CMe_3, 7). The alkylethynyl complexes **5–7** were prepared as previously described for the iron(II) phenyl- and (trimethylsilyl)ethynyl complexes **1** and **2**.[8] In a typical procedure, a 200-mL Schlenk flask equipped with a magnetic stirrer was charged with a solution of **4** (0.50 g, 0.47 mmol) in THF (50 mL) and a 10-fold excess of the appropriate terminal alkyne. The mixture was stirred for 15 min at reflux temperature; the initial pale yellow color turned light orange. Addition of ethanol (50 mL) and slow evaporation of the solvent gave orange crystals of the acetylides **5–7**.

GC analysis of the solutions revealed the formation of ca. 1 equiv of the corresponding alkene $H_2C{=}CHR$ (R = *n*-C_3H_7, *n*-C_5H_{11}, CMe_3). When **3** is substituted for **4**, 2 equiv of alkene are produced.

5: yield 90%; Λ_M = 44 Ω^{-1} cm^2 mol^{-1}; IR ν(C≡C) 2060 cm^{-1} (vw); μ_{eff} = 3.31 μ_B. Anal. Calcd for $C_{71}H_{69}BFeP_4$: C, 76.47; H, 6.14; Fe, 4.99. Found: C, 76.37; H, 6.21; Fe, 4.86.

6: yield 85%; Λ_M = 42 Ω^{-1} cm^2 mol^{-1}; IR ν(C≡C) 2065 cm^{-1} (vw); μ_{eff} = 3.37 μ_B. Anal. Calcd for $C_{73}H_{73}BFeP_4$: C, 76.85; H, 6.45; Fe, 4.89. Found: C, 76.78; H, 6.45; Fe, 4.80.

7: yield 90%; Λ_M = 41 Ω^{-1} cm^2 mol^{-1}; IR ν(C≡C) 2046 cm^{-1} (vw); μ_{eff} = 3.40 μ_B. Anal. Calcd for $C_{72}H_{71}BFeP_4$: C, 76.74; H, 6.35; Fe, 4.96. Found: C, 76.67; H, 6.32; Fe, 4.81.

Synthesis of the Iron(I) Alkynyls $[(PP_3)Fe(C{\equiv}CR)]$ (R = Ph, 8; $SiMe_3$, 9; *n*-C_3H_7, 10; *n*-C_5H_{11}, 11; CMe_3, 12). Method A. The parent iron(II)–alkynyl complex (ca. 0.50 mmol) dissolved in 30 mL of a THF solution containing 0.2 M $[NBu_4]ClO_4$ as supporting electrolyte was exhaustively electrolyzed at −1.0 V. At the end of the electrolysis, the orange solution turned deep red. Dark red crystals of $[(PP_3)Fe(C{\equiv}CR)]$ (R = Ph, **8**; $SiMe_3$, **9**; *n*-C_3H_7, **10**; *n*-C_5H_{11}, **11**; CMe_3, **12**) were obtained after addition of a 2-propanol/*n*-hexane mixture (30 mL, 2:1 v/v) and recrystallization from THF/2-propanol. Yield ca. 60%.

Method B. Solid cobaltocene (0.095 g, 0.50 mmol) was added with vigorous stirring to an orange THF solution (30 mL) of the appropriate iron(II)–alkynyl complex (ca. 0.50 mmol). Stirring was continued for 30 min. The color gradually turned to dark red and pale yellow needles of $[(C_5H_5)_2Co]BPh_4$ separated, which were filtered off. As a result, a clear red solution was obtained which, upon addition of a 2-propanol/*n*-hexane mixture (30 mL, 1:1 v/v), gave dark red crystals of the iron(I) alkynyls **8–12**. Yield ca. 90%.

8: IR ν(C≡C) 2030 cm^{-1} (s), phenyl reinforced vibration 1585 cm^{-1}; μ_{eff} = 2.10 μ_B. Anal. Calcd for $C_{50}H_{47}FeP_4$: C, 72.49; H, 5.72; Fe, 6.75. Found: C, 72.45; H, 5.79; Fe, 6.67.

9: IR ν(C≡C) 1962 cm^{-1} (s), ν(SiC) 855 cm^{-1} (s); μ_{eff} = 1.90 μ_B. Anal. Calcd for $C_{47}H_{51}FeP_4Si$: C, 68.53; H, 6.24; Fe, 6.78. Found: C, 68.44; H, 6.26; Fe, 6.65.

10: IR ν(C≡C) 2058 cm^{-1} (w); μ_{eff} = 2.05 μ_B. Anal. Calcd for $C_{47}H_{49}FeP_4$: C, 71.13; H, 6.22; Fe, 7.04. Found: C, 71.00; H, 6.27; Fe, 6.89.

11: IR ν(C≡C) 2057 cm^{-1} (vw); μ_{eff} = 2.15 μ_B. Anal. Calcd for $C_{49}H_{53}FeP_4$: C, 71.62; H, 6.50; Fe, 6.80. Found: C, 71.54; H, 5.51; Fe, 6.73.

12: IR ν(C≡C) 2043 cm^{-1} (w); μ_{eff} = 2.10 μ_B. Anal. Calcd for $C_{48}H_{51}FeP_4$: C, 71.38; H, 6.37; Fe, 6.91. Found: C, 71.28; H, 6.35; Fe, 6.88.

Reaction of $[(PP_3)Fe(C{\equiv}CR)]$ with $[(C_5H_5)_2Fe]PF_6$. Solid ferrocenium hexafluorophosphate (0.16 g, 0.47 mmol) was added with vigorous stirring to a CH_2Cl_2 solution (30 mL) of the appropriate iron(I)–alkynyl complex (**8–12**) to produce an orange solution from which the iron(II) alkynyls **1**, **2**, and **5–7** were obtained after addition of an ethanol solution (30 mL) of $NaBPh_4$ (0.43 g, 1.25 mmol).

X-ray Crystallographic Studies. A summary of crystal and intensity data for compounds **1** and **8** is presented in Table I. Experimental data were recorded at room temperature on Enraf-Nonius CAD4 (**1**) and Philips PW1100 (**8**) diffractometers using graphite-monochromated Mo Kα radiation. A set of 25 carefully centered reflections in the range $5.0 \le \theta \le 9.0$ and $8.0 \le \theta \le 10.5$ for **1** and **8**, respectively, was used for determining the lattice constants of each crystal. As a general procedure, the intensity of three standard reflections was measured periodically every 2 h. This procedure did not reveal an appreciable decay of intensities for either compound. The data were corrected for Lorentz, polarization, and absorption effects. The transmission factors ranged between 1.39 and 0.77 for **1** and between 0.94 and 0.93 for **8**. Atomic scattering factors were those tabulated by Cromer and Waber[13] with anomalous dispersion corrections taken from ref 14. The computational work was performed with the SHELX-76 system.[15]

Table I. Summary of Crystal Data for **8** and **1**

	8	**1**
formula	$C_{50}H_{47}P_4Fe_1$	$C_{78}H_{75}P_4O_1B_1Fe_1$
mol wt	827.67	1219.02
cryst dimension, mm	0.20 × 0.17 × 0.15	0.12 × 0.17 × 0.55
cryst system	monoclinic	monoclinic
space group	$P2_1/n$ (No. 14)	$P2_1/c$ (No. 15)
a, Å	14.560(3)	10.339(6)
b, Å	23.772(6)	33.259(9)
c, Å	12.334(4)	19.012(4)
β, deg	96.64(1)	92.13(3)
V, Å^3	4241.27	6533.04
Z	4	4
ρ_{calc}, g cm^{-3}	1.30	1.24
μ(Mo Kα), cm^{-1}	5.36	3.69
diffractometer	Phillips PW1100	CAD-4
radiation	graphite-monochromated Mo Kα, λ = 0.71069 Å	
scan type	ω–2θ	ω
$2q$ range, deg	5–46	5–40
scan width, deg	0.8 + 0.3(tan θ)	0.7 + 0.35(tan θ)
scan speed, deg s^{-1}	0.07	5.49
total data	6378	6377
unique data, $I > 3(\sigma)$	2550	2145
no. of parameters	165	228
R	0.061	0.079
R_w	0.068	0.079
abs corr: min, max	0.93–0.94	0.77–1.39

(10) Stoppioni, P.; Mani, F.; Sacconi, L. *Inorg. Chim. Acta* **1974**, *11*, 227.
(11) Smart, J. C.; Pinsky, B. L. *J. Am. Chem. Soc.* **1980**, *102*, 1009.
(12) Lozos, G. P.; Hoffman, G. B.; Franz, C. G. *SIM14A: Simulation of Powder EPR Spectra*; QCPE Program No. 265.
(13) Cromer, D. T.; Waber, J. T. *Acta Crystallogr.* **1965**, *18*, 104.
(14) *International Tables of Crystallography*; Kynoch Press: Birmingham, England, 1974.
(15) Sheldrick, G. M. *SHELX76 Program for Crystal Structure Determinations*; University of Cambridge: Cambridge, England, 1976.

Scheme I

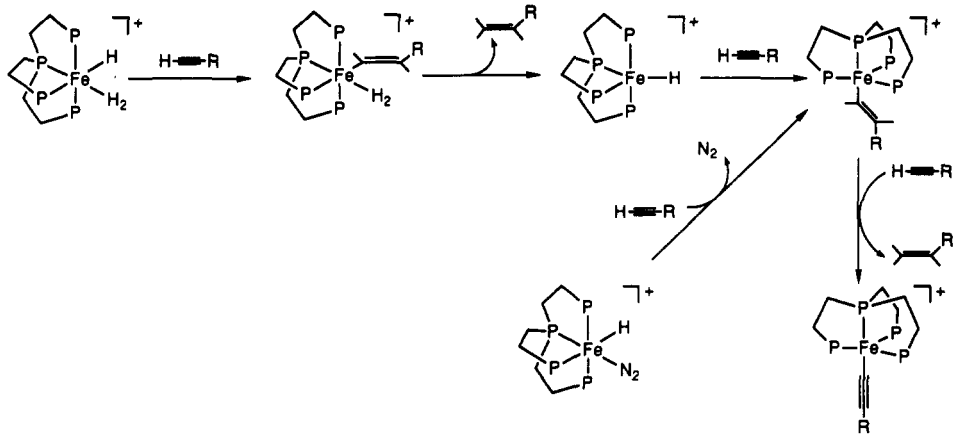

[(PP$_3$)Fe(C≡CPh)]BPh$_4$·C$_4$H$_8$O (1·THF). An orange parallelepiped crystal with dimensions of 0.12 × 0.17 × 0.55 mm was used for the data collection. The structure was solved by using heavy-atom and Fourier techniques. During the least-squares refinement Fe and P atoms were allotted anisotropic parameters. The phenyl rings were treated as rigid bodies with D_{6h} symmetry with C–C distances fixed at 1.39 Å and calculated hydrogen atom positions (C–H = 0.95 Å). Also, all atoms of the tetrahydrofuran ring were treated as carbon atoms. Final coordinates of all atoms are available as supplementary material.

[(PP$_3$)Fe(C≡CPh)] (8). A dark red parallelepiped crystal with dimensions of 0.20 × 0.17 × 0.15 mm was used for the data collection. The structure was solved by heavy-atom and Fourier techniques. Anisotropic thermal parameters were used only for the iron and phosphorus atoms. As for the parent compound **1**, the phenyl rings were treated as rigid bodies with D_{6h} symmetry (C–C = 1.39 Å) and hydrogen atoms were introduced at calculated positions (C–H = 0.95 Å). Final coordinates of all atoms are available as supplementary material.

Results and Discussion

Synthesis and Characterization of the Iron(II)–Alkynyl Complexes. The novel iron(II) alkynyls [(PP$_3$)Fe(C≡CR)]BPh$_4$ (R = *n*-C$_3$H$_7$, **5**; *n*-C$_5$H$_{11}$, **6**; CMe$_3$, **7**) have been prepared by a procedure which had successfully been employed for the synthesis of **1** and **2**.[8] This involves the reaction of either the η^2-H$_2$ complex [(PP$_3$)Fe(H)(H$_2$)]BPh$_4$ (**3**) or the dinitrogen derivative [(PP$_3$)Fe(H)(N$_2$)]BPh$_4$ (**4**) in THF with an excess of the appropriate terminal alkyne at reflux temperature. In all cases, depending on the use of either **3** or **4**, 1 or 2 equiv of the corresponding alkene are formed. A detailed description of the reactions leading to the novel Fe(II) acetylides is not in order, as they definitely proceed through a stepwise mechanism previously established for the synthesis of **1**, **2**, and the related Ru(II) complex [(PP$_3$)Ru(C≡CSiMe$_3$)]BPh$_4$ (Scheme I).[16]

All iron(II) alkynyls exhibit quite similar chemicophysical properties. They are orange crystalline products that are air stable in both the solid state and solution (halogenated solvents, acetone, THF, and nitroethane), where they behave as 1:1 electrolytes. All compounds are paramagnetic with μ_{eff} values ranging from 3.28 to 3.42 μ_B at room temperature. Such values correspond to two unpaired spins and, therefore, indicate a low-spin trigonal-bipyramidal (TBP) d^6 electronic configuration, which is typical for Fe(II) complexes with the PP$_3$ ligand.[17]

The IR spectra show very weak ν(C≡C) bands in the 2060–2035-cm^{-1} region, which, in some cases, are matched by strong Raman absorptions.[8] The stretching vibration of the C≡C bond (1990 cm^{-1}) exhibits the expected strong intensity in the (trimethylsilyl)acetylide complex **2** only.

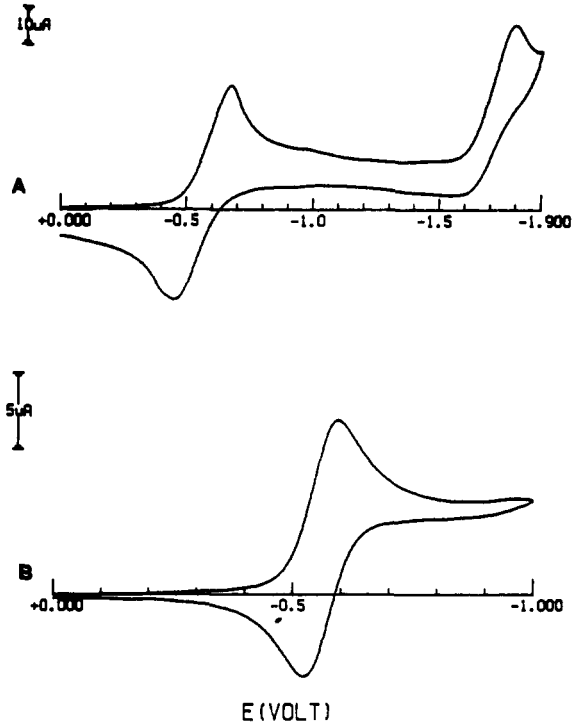

Figure 1. Cyclic voltammograms recorded at a mercury electrode on a deaerated tetrahydrofuran solution containing **1** (1.61 × 10^{-3} mol dm^{-3}) and (NBu$_4$)(ClO$_4$) (0.2 mol dm^{-3}) at a scan rate of (A) 0.2 and (B) 0.02 V s^{-1}.

Redox Properties of the Iron(II) Acetylides. All iron(II)–alkynyl complexes undergo electron-transfer reactions that encompass the Fe(I), Fe(II), and Fe(III) oxidation states of the metal.

As an example, the cyclic voltammetric response exhibited by **1** in THF is reported in Figure 1, while the most relevant parameters for the redox changes exhibited by all other complexes are summarized in Table II.

Two successive reduction steps are displayed, only the first one exhibiting features of chemical reversibility. Controlled potential coulometry (E_w = −1.0 V) showed that the first electron addition process involves one electron/molecule.

Analysis[18] of the cyclic voltammetric responses of the first cathodic process recorded at a mercury electrode with scan rate v varying from 0.02 to 5.12 V s^{-1} indicates that (i) the peak current ratio $i_{p(backward)}/i_{p(forward)}$ is constantly equal to unity, (ii) the current function $i_{p(forward)}v^{-1/2}$ remains substantially constant

(16) Bianchini, C.; Peruzzini, M.; Zanobini, F.; Frediani, P.; Albinati, A. *J. Am. Chem. Soc.* **1991**, *113*, 5453.

(17) (a) Bacci, M.; Midollini, S.; Stoppioni, L.; Sacconi, L. *Inorg. Chem.* **1973**, *12*, 1801. (b) Sacconi, L.; Di Vaira, M. *Inorg. Chem.* **1978**, *17*, 810. (c) Di Vaira, M.; Midollini, S.; Sacconi, L. *Inorg. Chem.* **1977**, *16*, 1518.

(18) Brown, E. R.; Sandifer, J. *Physical Methods of Chemistry. Electrochemical Methods*; Rossiter, B. W., Hamilton, J. F., Eds.; Wiley Interscience: New York, 1986; Vol. II, Chapter 4.

Table II. Formal Electrode Potentials (V) and Peak-to-Peak Separation (mV) for the $[(PP_3)Fe(C{\equiv}CR)]^{+/0}$ Redox Change

R	$E^{\circ\prime}$	ΔE_p[a]	ΔE_p[b]	solvent
C_6H_5	-0.59	126	109	THF
	-0.71	82	70	CH_2Cl_2
$SiMe_3$	-0.58	228		THF
n-C_3H_7	-0.69	230		THF
n-C_5H_{11}	-0.68	244		THF
CMe_3	-0.67	98		THF

[a] Measured at a platinum electrode, at 0.2 V s^{-1}. [b] Measured at a mercury electrode, at 0.2 V s^{-1}.

in the range from 0.02 to 1.00 V s^{-1} and then it slightly decreases, and (iii) the peak-to-peak separation (ΔE_p) increases progressively from 67 to 402 mV.

In strongly resistive solvents, particularly at high scan rates, uncompensated solution resistances are usually responsible for the departure of the peak-to-peak separation from the constant value of 59 mV (expected for an electrochemically reversible one-electron transfer). It is therefore reasonable to conclude that a simple one-electron reduction has occurred, which slightly departs from pure electrochemical reversibility. In contrast, Figure 1 clearly shows the instability of the iron(0) monoanion $[(PP_3)Fe(C{\equiv}CPh)]^-$, which is generated in correspondence to the second cathodic peak.

In summary, the iron(I) complex $[(PP_3)Fe(C{\equiv}CPh)]$ and the other Fe(I) alkynyls as well appear sufficiently stable to be synthesized by electrochemical or chemical reduction of the parent Fe(II) derivatives. Furthermore, the near electrochemical reversibility of the $[(PP_3)Fe(C{\equiv}CPh)]^{+/0}$ electron transfer suggests that minor geometrical reorganizations accompany the redox change.[19]

The use of electrochemical techniques to generate iron(I) species by one-electron reduction of Fe(II) derivatives is a well-known procedure. In particular, after Dessy's seminal work,[20] many studies have dealt with the one-electron reduction of $[(\eta^5\text{-}C_5H_5)Fe(\eta^6\text{-arene})]^+$ complexes, and the multiple aspects of the reactivity of the electrogenerated corresponding Fe(I) species have been elucidated.[21-24] Also, the one-electron reduction of the bis(arene) derivatives $[Fe(\eta^6\text{-arene})_2]^{2+}$ [25] and the sequential reduction Fe(III)/Fe(II)/Fe(I)/Fe(0) of iron porphyrins have been reported.[26] In contrast, the synthesis of Fe(I) compounds via one-electron oxidation of Fe(0) derivatives has received little attention.[27] Finally, as a confirmation of the aptitude of tripodal polyphosphine ligands to stabilize metal complexes in low oxidation states,[7b,c] it is worth mentioning that the octahedral Fe(II) σ-alkynyl complex $[FeCl(DMPE)_2(C{\equiv}CPh)]$ [DMPE = bis(dimethylphosphino)ethane] does not undergo reduction to the Fe(I) derivative, whereas the stable Fe(III) congener is readily obtained by one-electron oxidation.[28]

Table III. Selected Bond Distances (Å) and Angles (deg) for **1** and **8**

	1	**8**		**1**	**8**
Fe-P1	2.315(6)	2.214(3)	P1-Fe-C7	98.8(6)	103.0(3)
Fe-P2	2.292(6)	2.212(3)	P2-Fe-C7	100.1(6)	94.5(3)
Fe-P3	2.301(6)	2.187(3)	P3-Fe-C7	94.8(6)	90.4(3)
Fe-P4	2.225(6)	2.153(3)	P4-Fe-C7	177.2(6)	170.3(3)
Fe-C7	1.88(2)	1.92(1)	P1-Fe-P2	115.6(2)	111.1(1)
P1-C1	1.87(2)	1.85(1)	P1-Fe-P3	119.4(2)	102.4(1)
P2-C3	1.83(2)	1.83(1)	P1-Fe-P4	82.4(2)	86.3(1)
P3-C5	1.85(2)	1.85(1)	P2-Fe-P3	119.4(2)	143.9(1)
P4-C2	1.84(2)	1.83(1)	P2-Fe-P4	81.5(2)	84.5(1)
P4-C4	1.75(2)	1.84(1)	P3-Fe-P4	82.4(2)	84.8(1)
P4-C6	1.82(2)	1.82(1)	Fe-C7-C8	175(2)	173.8(9)
C7-C8	1.20(3)	1.21(1)	C7-C8-C1,7	177(2)	174(1)
C8-C1,7	1.47(3)	1.45(1)			

Synthesis and Characterization of the Iron(I)-Alkynyl Complexes. In keeping with the cyclic voltammetric responses, exhaustive macroelectrolysis experiments at -1.0 V of the iron(II) acetylides in either CH_2Cl_2 or THF produce dark red solutions from which the corresponding Fe(I) alkynyls $[(PP_3)Fe(C{\equiv}CR)]$ (R = Ph, **8**; $SiMe_3$, **9**; n-C_3H_7, **10**; n-C_5H_{11}, **11**; CMe_3, **12**) can be isolated in ca. 60% yield. Alternatively, compounds **8-12** can be prepared in higher yields (up to 90%) by chemical reduction of the Fe(II) acetylides dissolved in THF with a stoichiometric amount of cobaltocene (eq 1).

$$[(PP_3)Fe(C{\equiv}CR)]BPh_4 + [Cp_2Co] \rightarrow [(PP_3)Fe(C{\equiv}CR)] + [Cp_2Co]BPh_4 \quad (1)$$

Compounds **8-12** are stable in the solid state and in solutions where they behave as nonelectrolytes. The presence of terminal alkynyl ligands is clearly shown by IR bands of medium to strong intensity in the 2060-1960-cm^{-1} region. With the exception of the (trimethylsilyl)ethynyl complex **9**, the $\nu(C{\equiv}C)$ bands in the Fe(I) compounds are practically unshifted with respect to those of the Fe(II) congeners. In contrast, **9** exhibits a strong intensity band (1962 cm^{-1}) shifted to lower wavenumber by ca. 30 cm^{-1} as compared to the iron(II) alkynyl **2**.

All iron(I) alkynyls are paramagnetic with bulk magnetic moments ranging from 1.90 to 2.15 μ_B. These values well match those reported for other iron(I) complexes (from 1.80 to 2.30 μ_B) and are diagnostic of the presence of one unpaired spin (d^7 low-spin configuration of the metal).[29-31]

Molecular Structures of the Iron(I)- and Iron(II)-Phenylethynyl Complexes. The molecular structures of **1** and **8** have been determined by single-crystal X-ray diffraction analyses. Selected bond lengths and angles are listed in Table III. ORTEP drawings for **1** and **8** are reproduced in Figures 2 and 3, respectively, together with atomic labeling schemes.

Both compounds consist of discrete monomeric complexes. Each metal center is surrounded by five donor atoms in a trigonal-bipyramidal environment, which is almost regular in **1**, but largely distorted in **8**. The three peripheral P atoms of the polyphosphine occupy the equatorial positions while the bridgehead phosphorus atom and the phenyethynyl ligand are located trans to each other in the axial positions. Tetraphenylborate anions and chlathrated THF molecules in a 1:1 ratio complete the molecular structure of the cationic complex **1**.

(19) Zanello, P. In *Stereochemistry of Organometallic and Inorganic Compounds*; Bernal, I., Ed.; Elsevier: Amsterdam, 1990; Vol. 4, p 191.
(20) Dessy, R. E.; Stary, F. E.; King, R. B.; Waldrop, M. *J. Am. Chem. Soc.* **1966**, *88*, 471.
(21) Morrison, W. H.; Ho, E. Y.; Hendrickson, D. N. *Inorg. Chem.* **1975**, *14*, 500.
(22) (a) Astruc, D.; Dabard, R. *Bull. Soc. Chim. Fr.* **1976**, 228. (b) Astruc, D.; Roman, E.; Hamon, J.-R.; Batail, P. *J. Am. Chem. Soc.* **1979**, *101*, 2240. (c) Astruc, D.; Hamon, J.-R.; Althoff, G.; Roman, E.; Batail, P.; Michaud, P.; Mariot, J.-P.; Varret, F.; Cozak, D. *J. Am. Chem. Soc.* **1979**, *101*, 5445. (d) Moinet, C.; Roman, E.; Astruc, D. *J. Electroanal. Chem.* **1981**, *121*, 241. (e) Hamon, J.-R.; Astruc, D.; Michaud, P. *J. Am. Chem. Soc.* **1981**, *103*, 758. (f) Hamon, J.-R.; Astruc, D.; Roman, E.; Batail, P.; Mayerle, J. J. *J. Am. Chem. Soc.* **1981**, *103*, 2431. (g) Astruc, D. *Tetrahedron* **1983**, *39*, 4027. (h) Ruiz, J.; Guerchais, V.; Astruc, D. *J. Chem. Soc., Chem. Commun.* **1989**, 812.
(23) Buet, A.; Darchen, A.; Moinet, C. *J. Chem. Soc., Chem. Commun.* **1979**, 447.
(24) (a) El Murr, N. *J. Chem. Soc., Chem. Commun.* **1981**, 251. (b) Darchen, A. *J. Chem. Soc., Chem. Commun.* **1983**, 768. (c) Darchen, A. *J. Organomet. Chem.* **1986**, *302*, 389.
(25) Braitsh, D. M.; Kumarappan, R. *J. Organomet. Chem.* **1975**, *84*, C37.
(26) (a) Croisy, A.; Lexa, D.; Momenteau, M.; Saveant, J.-M. *Organometallics* **1985**, *4*, 1574. (b) Guetin, C.; Lexa, D.; Momenteau, M.; Saveant, J.-M. *J. Am. Chem. Soc.* **1990**, *112*, 1874.
(27) Connelly, N. G.; Somers, K. R. *J. Organomet. Chem.* **1976**, *113*, C39.
(28) Field, L. D.; George, A. V.; Laschi, F.; Malouf, E. Y.; Zanello, P. *J. Organomet. Chem.* **1992**, *435*, 347.
(29) (a) Gargano, M.; Giannocaro, P.; Rossi, M.; Sacco, A. *J. Chem. Soc., Chem. Commun.* **1973**, 223. (b) Giannocaro, P.; Sacco, A. *Inorg. Synth.* **1977**, *17*, 71. (c) Gargano, M.; Giannocaro, P.; Rossi, M.; Vasapollo, G.; Sacco, A. *J. Chem. Soc., Dalton Trans.* **1975**, 9.
(30) Lappert, M. F.; MacQuitty, J. J.; Pye, P. L. *J. Chem. Soc., Dalton Trans.* **1981**, 1583.
(31) Rakowsky, M. C.; Busch, D. H. *J. Am. Chem. Soc.* **1975**, *97*, 2570.

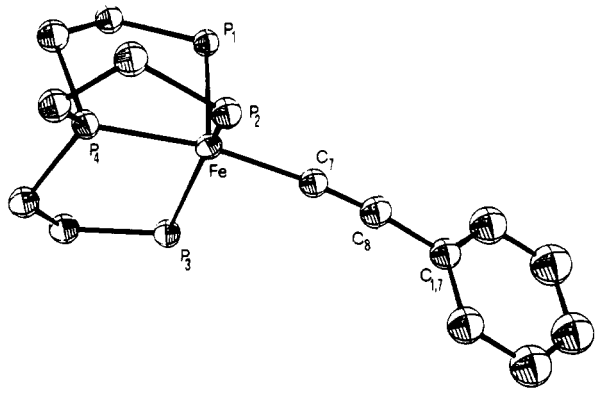

Figure 2. ORTEP drawing of $[(PP_3)Fe(C{\equiv}CPh)]$ (**8**). Phenyl rings of the PP_3 ligand have been omitted for the sake of clarity.

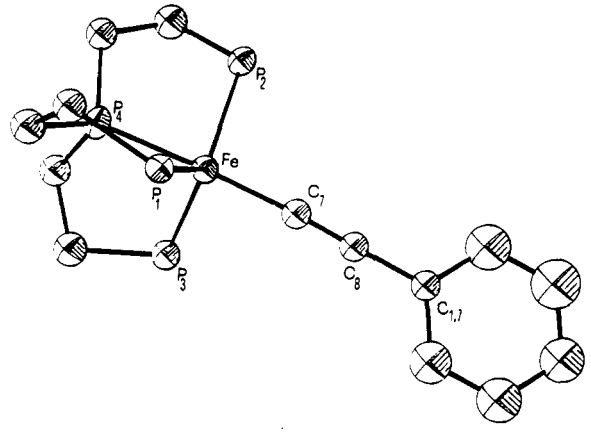

Figure 3. ORTEP drawing of the $[(PP_3)Fe(C{\equiv}CPh)]^+$ complex cation (**1**). Phenyl rings of the PP_3 ligand have been omitted for the sake of clarity.

Inspection of the structural data readily shows that the one-electron reduction of **1** to **8** significantly affects the bonding pattern within the "$Fe(PP_3)$" moiety. In particular, we note a decrease of the average Fe–P distance by 0.09 Å. A slight increase of the iron to ethynyl carbon (C_7) distance from 1.88(2) to 1.92(1) Å is also observed, which, however, must be handled with caution. The variation of the bond lengths within the "$Fe(PP_3)$" fragment of the redox couple **1**/**8** correlate well with literature data on redox-related metal polyphosphine complexes.[32-34] As suggested by Orpen and Connelly,[35] the decrease in the Fe–P bond distances on going from **1** to **8** can be rationalized in terms of a significant metal → phosphorus π-back-bonding contribution. In effect, the reduction of a complex is expected to increase the π-donor abilities of the metal center, thus inducing a strengthening of the chemical bonds to π-acceptor ligands.[36]

Major structural differences in the geometries of **1** and **8** involve the P–Fe–P bond angles in the equatorial plane of the trigonal bipyramid. A perusal of the crystallographic data reveals that while the equatorial angles in the iron(II) complex **1** (ranging from 115.6(2)° to 119.4(2)°) well match the value expected for a dsp^3 hybridization of the metal ion, the corresponding angles in the reduced iron(I) complex diverge from such values. In

Scheme II

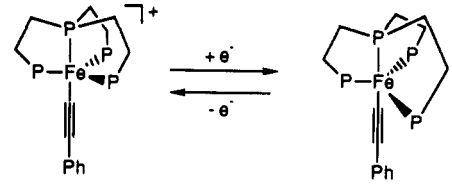

particular, in going from **1** to **8**, the P_1–Fe–P_2 and P_1–Fe–P_3 angles reduce from 115.6(2)° and 119.4(2)° to 111.1(1)° and 102.4(1)°, respectively, and the equatorial angle P_2–Fe–P_3 opens from 119.4(2)° up to 143.9(1)°.

Similar distortions have been reported for Co(II) complexes[37] stabilized by the tripodal tetradentate phosphines PP_3 and NP_3 [$NP_3 = N(CH_2CH_2PPh_2)_3$] and have been rationalized in terms of Jahn–Teller effect.[38,7b,c] In fact, for a 17-electron system in a trigonal-bipyramidal environment a Jahn–Teller distortion is expected to ensue, leading to a more or less pronounced breakdown of the molecular symmetry. A case in point is provided by the present iron(I)–alkynyl complex in which the extra electron causes a lowering of the C_{3v} symmetry of the parent iron(II) derivative. Indeed, the three-atom sequence P_4–Fe–C_7 is almost linear in **1** [177.2(6)°], but deviates significantly from linearity in **8** [170.3(3)°], i.e. appreciable bending of the iron–alkynyl fragment toward the cradle of the opened P_2–Fe–P_3 angle has occurred.

A perusal of the structural data for **1** and **8** reveals that the C≡C triple bond lengths in the two alkynyl complexes [1.20(1) Å for **8** vs. 1.21(1) Å for **1**] do not differ significantly from those found in either organic alkynes (ca. 1.20 Å)[39] or metallorganic acetylides (1.18–1.25 Å).[7,40,41] Finally, the bond distance between the ethynyl ligand and the ipso carbon of the phenyl ring is almost identical in **1** and **8** [1.45(1) and 1.47(3) Å, respectively] and practically corresponds to the sum of the covalent radii for aromatic [$C(sp^2)$ = 0.75 Å] and acetylenic [C(sp) = 0.65–0.70 Å] carbon atoms.[42]

From a comparison of the bonding pattern within the Fe—C≡CPh moiety in the redox couple **1**/**8**, one readily infers that metal to alkynyl ligand back-donation does not contribute to describe the Fe—C≡C bond in **8**. In fact, it is well established that an effective transfer of electrons from the metal to the alkynyl ligand increases the M–C bond order and decreases the C–C bond order.[43] Ultimately, a significant $d\pi(\text{metal}) \rightarrow \pi^*(\text{alkynyl})$ interaction in the HOMO would drive the C≡C stretching frequency down. None of these experimental observables is found in going from **1** to its electron-richer derivative **8**. Indeed, the Fe–C_7 bond length slightly increases, while both the C≡C bond distance and ν(C≡C) remain practically constant. Since no appreciable variation of ν(C≡C) is observed for all other Fe(I)/Fe(II) σ-alkynyl couples described in this paper, except the trimethylsilyl derivatives (see below), one may conclude that in

(32) (a) $[(PP_3)CoH]BF_4$: Orlandini, A.; Sacconi, L. *Cryst. Struct. Commun.* **1975**, *4*, 157. (b) $[(PP_3)CoH]$: Ghilardi, C. A.; Sacconi, L. *Cryst. Struct. Commun.* **1975**, *4*, 149.

(33) (a) [(triphos)NiI]: Dapporto, P.; Fallani, G.; Sacconi, L. *Inorg. Chem.* **1974**, *13*, 2847. (b) $[(triphos)NiI]_2[As_6I_8]$: Zanello, P.; Cinquantini, A.; Ghilardi, C. A.; Midollini, S.; Moneti, S.; Orlandini, A.; Bencini, A. *J. Chem. Soc., Dalton Trans.* **1990**, 3761. triphos = $MeC(CH_2PPh_2)_3$.

(34) (a) $[(NP_3)NiI]I$: Dapporto, P.; Sacconi, L. *J. Chem. Soc., A* **1970**, 1804. (b) $[(NP_3)NiI]$: Dapporto, P.; Sacconi, L. *Inorg. Chim. Acta* **1980**, *39*, 61. $NP_3 = N(CH_2CH_2PPh_2)_3$.

(35) Orpen, A. G.; Connelly, N. G. *Organometallics* **1990**, *9*, 1206.

(36) Beddoes, R. L.; Bitcon, C.; Whiteley, M. W. *J. Organomet. Chem.* **1991**, *402*, 85.

(37) (a) Sacconi, L.; Ghilardi, C. A.; Mealli, C.; Zanobini, F. *Inorg. Chem.* **1975**, *14*, 1380. (b) Sacconi, L.; Orlandini, A.; Midollini, S. *Inorg. Chem.* **1974**, *13*, 2850. (c) Cecconi, F.; Ghilardi, C. A.; Midollini, S.; Moneti, S.; Orlandini, S.; Scapacci, G. *J. Chem. Soc., Dalton Trans.* **1989**, 211. (d) Mealli, C.; Sacconi, L. *J. Chem. Soc., Chem. Commun.* **1973**, 886. (e) Ghilardi, C. A.; Midollini, S.; Moneti, S.; Orlandini, A. *J. Chem. Soc., Chem. Commun.* **1986**, 1771.

(38) Mealli, C.; Ghilardi, C. A.; Orlandini, A. *Coord. Chem. Rev.* **1992**, *120*, 361.

(39) March, J. W. *Advanced Organic Chemistry*; Wiley Interscience: New York, 1985.

(40) Akita, M.; Terada, M.; Oyama, S.; Moro-oka, Y. *Organometallics* **1990**, *9*, 816 and references therein.

(41) For other X-ray authenticated Fe(II) phenylethynyl complexes see: (a) Goddard, R.; Howard, J.; Woodward, P. *J. Chem. Soc., A* **1974**, 2025. (b) Bruce, M. I.; Clark, R.; Howard, J.; Woodward, P. *J. Organomet. Chem.* **1972**, *42*, C107. (c) Gamasa, M. P.; Gimeno, J.; Lanfranchi, M.; Tiripicchio, A. *J. Organomet. Chem.* **1991**, *405*, 333. (d) Field, L.; George, A. W.; Malouf, E. Y.; Slip, I. H. M.; Hambley, T. W. *Organometallics* **1991**, *10*, 3842.

(42) Cotton, F. A.; Wilkinson, G. *Advanced Inorganic Chemistry*, 3rd ed.; Wiley Interscience: London, 1972; p 117. Elschenbroich, C.; Salzer, A. *Organometallics*; Verlag Chemie: Weinheim, Germany, 1989.

(43) Kostic, N. M.; Fenske, R. F. *Organometallics* **1982**, *1*, 974.

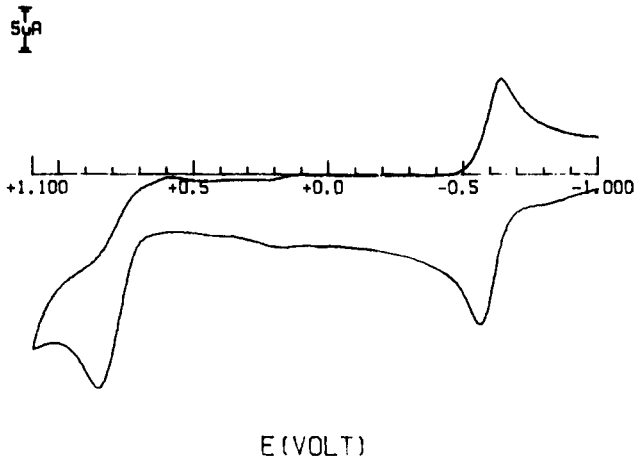

Figure 4. Cyclic voltammogram recorded at a platinum electrode on a deaerated tetrahydrofuran solution containing **8** (1.21×10^{-3} mol dm^{-3}) and $(NBu_4)(ClO_4)$ (0.2 mol dm^{-3}) at a scan rate of 0.2 V s^{-1}.

the present Fe(I) alkynyls, and even more so in the Fe(II) derivatives, no significant electron transfer from metal to alkynyl ligand occurs. This finding seemingly contrast with previous reports on related trigonal-bipyramidal complexes of the general formula $[(PP_3)M(C{\equiv}CR)]$ (M = Co, Rh; R = Ph, CO_2Et) for which a significant $d\pi$(metal) $\rightarrow \pi^*$(alkynyl) interaction was suggested on the basis of the $\nu(C{\equiv}C)$ values and the redox potentials relative to the stepwise one-electron oxidation sequence M(I)/M(II)/M(III).[7b,c] The different behavior of iron(I) vs. cobat(I) or rhodium(I) may be rationalized by recalling that the metal to ligand electron transfer in σ-alkynyl complexes may be scarce or even absent because of the high energy of the π^* level of the alkynyl.[36,44] Accordingly, $d\pi$(metal) $\rightarrow \pi^*$(alkynyl) transfer is favored for late transition metals, preferentially in a low oxidation state, as well as for alkynyl substituents with electron-withdrawing character. In this light the anomalous behavior of the (trimethylsilyl)alkynyl complexes **2** and **9** which exhibit the lowest $\nu(C{\equiv}C)$ values of the series (1990 and 1962 cm^{-1}, respectively) may be interpreted in terms of a remarkable electron-withdrawing capability of the trimethylsilyl group when bonded to a C–C triple bond. The reasons for this behavior are difficult to assess in the absence of a detailed theoretical analysis. However, it is worth reporting that silyl substituents are known to stabilize carboanions as well as to decrease the bond order of carbonyl groups in the α position.[45]

Redox Properties of the Iron(I) Acetylides. Figure 4 illustrates the anodic pathway of **8** in THF solution. The cyclic voltammogram shows not only the expected Fe(I)/Fe(II) reversible oxidation but also the further Fe(II)/Fe(III) oxidative step (E_p = +0.86 V), which, in the experimental conditions of Figure 1, was difficult to detect because of the concomitant presence of the oxidizable tetraphenylborate counteranion. Like the Fe(I)/Fe(0) reduction, the Fe(II)/Fe(III) redox change is irreversible in character. Qualitatively similar results are observed for all iron(I) acetylides and are summarized in Table II.

X-Band ESR Characterization of the Fe(I)- and Fe(II)–Alkynyl Complexes. The relative insensitivity of the redox potentials to the electronic effects of the alkyne substituents together with the nature of the major structural changes suggests that the electron added to the Fe(II) alkynyls enters a bonding orbital which is largely centered on the iron polyphosphine moiety. This idea is strongly supported by the ESR properties of the Fe(I) alkynyls.

Powder Spectra. Fe(I) Complexes. Figure 5a shows the powder X-band ESR spectrum of **8** at 100 K. The line-shape analysis has been interpreted in terms of a $S = {}^1/_2$ spin Hamiltonian

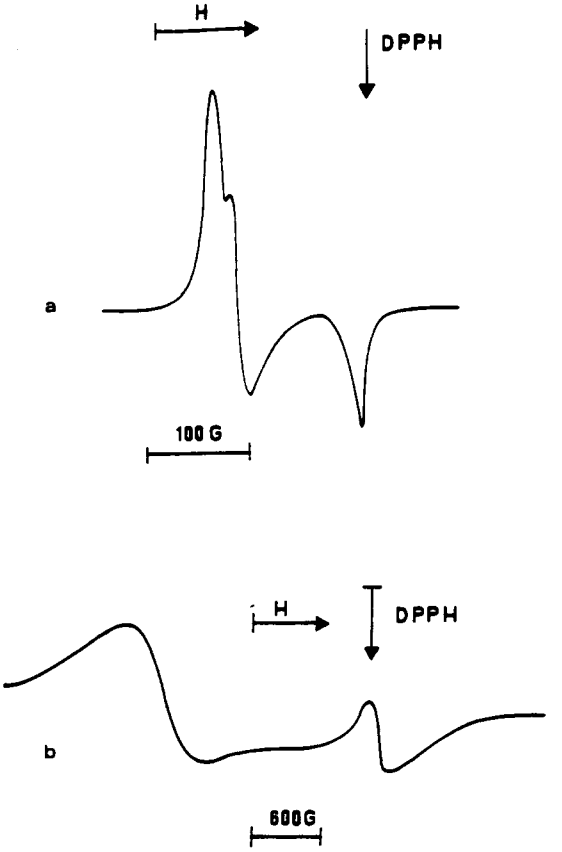

Figure 5. (a) Powder X-band ESR spectrum of **8** at 100 K. (b) Powder X-band ESR spectrum of **1** at 100 K.

resulting from the electronic structure of a Fe(I) ion in a distorted TBP coordination polyhedron. The well-resolved absorption pattern exhibits rhombic structure with the following anisotropic parameters: $g_l = 2.104$, $g_m = 2.081$, $g_h = 2.005$ [$\langle g_{calcd} \rangle = {}^1/_3(g_l + g_m + g_h) = 2.063$]. The lack of hyperfine splittings due to magnetic interaction between the unpaired electron and the phosphorus nuclei ($I = {}^1/_2$) of the PP_3 ligand is not surprising because of spin–spin exchange narrowing processes occurring at sufficiently fast rates in the solid state to obliterate the hyperfine structure of the phosphorus nuclei.[46,47] The second derivative spectrum is poorly resolved and allows one to settle only an upper-limit value of the a_P coupling constant: $\Delta H(100\ K) = 30\ G \geq a_P$. On the other hand, the ESR evidence for three g_i values indicates that significant asymmetry in the Fe(I) coordination polyhedron is experienced by the unpaired electron, a result that agrees with the X-ray analysis. As the temperature is increased, the line shape of the signal maintains the anisotropic features, while it slightly broadens, indicating that an increase in the temperature moderately affects the powder electron-spin relaxation times.[46,47]

Quite similar ESR parameters are exhibited by all Fe(I) alkynyls even though minor variations of the g_i parameters are observed depending on the nature of the alkynyl substituent (Table IV). In particular, inspection of the powder data shows that the rhombic structure is shared by all compounds over a temperature range as large as 200 K.

Fe(II) Complexes. The powder ESR spectrum of the Fe(II) derivative **1** at 100 K consists of two unresolved signals (Figure 5b). The relevant parameters are $g_m = 4.280$, $\Delta H_m = 750$ G and $g_h = 1.976$, $\Delta H_h = 95$ G. An increase in the temperature to 300 K induces the disappearance of both absorption signals, which,

(44) Adams, J. S.; Bitcon, C.; Brown, J. R.; Collison, D.; Cunningham, M.; Whiteley, M. W. *J. Chem. Soc., Dalton Trans.* **1987**, 3049.
(45) (a) Grev, R. S.; Schaefer, H. F., III *J. Am. Chem. Soc.* **1989**, *111*, 6137. (b) Wetzel, D. M.; Brauman, J. I. *J. Am. Chem. Soc.* **1988**, *110*, 8333.
(46) Carrington, A.; McLachlan, A. D. *Introduction to Magnetic Resonance*; Harper International: New York, 1967.
(47) Goodman, B. A.; Raynor, J. B. Electron Spin Resonance of Transition Metal Complexes. In *Adv. Inorg. Chem. Radiochem.* **1970**, *13*.

Table IV. X-Band EPR Parameters for the Iron(I) Alkynyls

R	state[a]	g_l[b]	g_m[b]	g_h[b]	$\langle g_{calcd}\rangle$[b,c]	$\langle g\rangle$[b]	$\langle a\rangle$[d]
Ph	$A_{(230\ K)}$					2.066	44
							16
	$A_{(300\ K)}$					2.064	≤16
	$B_{(100\ K)}$	2.104	2.081	2.005	2.063		
	$B_{(300\ K)}$	2.106	2.084	2.007	2.066		
$SiMe_3$	$A_{(230\ K)}$					2.067	43
							17
	$A_{(300\ K)}$					2.064	14
	$B_{(100\ K)}$	2.102	2.078	2.008	2.063		
	$B_{(300\ K)}$	2.100	2.077	2.011	2.063		
C_3H_7	$A_{(230\ K)}$					2.064	48
							17
	$A_{(300\ K)}$					2.064	15
	$B_{(100\ K)}$	2.105	2.072	2.005	2.061		
	$B_{(300\ K)}$	2.109	2.072	2.006	2.063		
C_5H_{11}	$A_{(100\ K)}$[e]					2.066	47
							18
	$A_{(300\ K)}$					2.065	13
	$B_{(100\ K)}$	2.099	2.072	2.002	2.058		
	$B_{(300\ K)}$	2.101	2.070	2.002	2.058		
CMe_3	$A_{(230\ K)}$					2.065	48
							16
	$A_{(300\ K)}$					2.063	14
	$B_{(100\ K)}$	2.101	2.080	2.009	2.063		
	$B_{(300\ K)}$	2.102	2.080	2.010	2.064		

[a] A, THF solution; B, powder. [b] g values are expressed with an error of ±0.005. [c] $\langle g_{calcd}\rangle$ values are obtained from the formula $\langle g\rangle = 1/3\cdot(g_l + g_m + g_h)$. [d] $\langle a\rangle$ and ΔH_{av} are expressed with an error of ±5 G. [e] Recorded in 2-methyltetrahydrofuran, see text.

Table V. X-Band EPR Parameters for the Iron(II) Alkynyls

R[a]	state[b]	g_l[c]	ΔH_l[d]	g_m[c]	ΔH_m[d]	g_h[c]	ΔH_h[d]
Ph	$A_{(100\ K)}$	e					
	$A_{(300\ K)}$	e					
	$B_{(100\ K)}$			4.280	≈750	1.976	95
	$B_{(300\ K)}$	e					
C_3H_7	$A_{(100\ K)}$	9.910	100	4.285	90	1.980	≈250
	$A_{(300\ K)}$	e					
	$B_{(100\ K)}$	9.890	90	4.305	90	1.980	≈270
	$B_{(300\ K)}$	9.900	150	4.320	150	1.950	≈450
C_5H_{11}	$A_{(100\ K)}$			4.238	110		
	$A_{(300\ K)}$	e					
	$B_{(100\ K)}$			4.348	85	2.048	100
	$B_{(300\ K)}$	e					
CMe_3	$A_{(100\ K)}$	9.425	≈180	4.305	80		
	$A_{(300\ K)}$	e					
	$B_{(100\ K)}$	9.830	100	4.300	130	2.010	≈450
	$B_{(300\ K)}$	9.910	95	4.350	150	1.960	≈600

[a] No data are available for the trimethylsilylethynyl complex **9**. [b] A, THF solution; B, powder. [c] g values are expressed with an error of ±0.005. [d] ΔH values are expressed with an error of ±5 G. [e] No signal was detected in the field range 0–6000 G.

however, reversibly emerge from the baseline as the temperature is decreased. This finding can be explained assuming the presence of a paramagnetic metal ion with a total spin quantum number $S > 1/2$. In the case at hand, as indicated also by the experimental μ_{eff} values, a $S = 1$ spin Hamiltonian can be taken into account to explain both the effective temperature dependence of the Fe(II) powder spectra and the occurrence of the intense low-field absorptions at liquid nitrogen temperature. As shown in Table V, the powder ESR spectra of all of the Fe(II) compounds display similar spectral features. The nature of the alkynyl substituent affects the relevant spectral parameters, particularly those at 100 K, to a larger extent than is observed for the corresponding Fe(I) derivatives, due to an active zero-field splitting term in the $S = 1$ Hamiltonian.[46-48]

In summary, the powder spectra of the Fe(II) alkynyls are consistent with a d^6 low-spin configuration of the metal in an almost regular TBP environment.[49]

(48) McGarvey, B. R. *Transition Met. Chem. (N.Y.)* **1966**, *3*, 89.

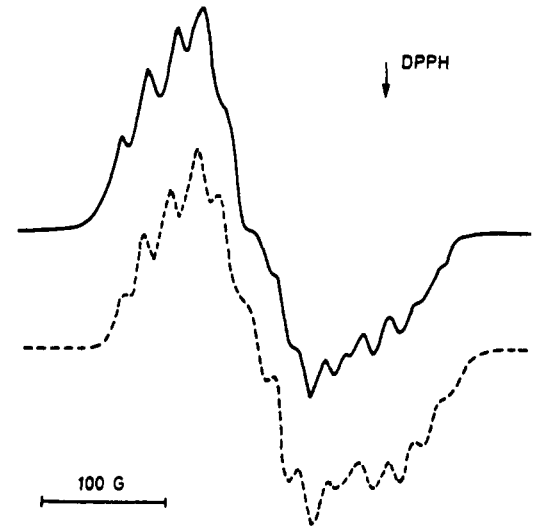

Figure 6. Experimental (full line) and computed (dashed line) X-band ESR spectra at 100 K of **11** dissolved in 2-methyltetrahydrofuran.

Fluid and Frozen Solution Spectra. Fe(I) Complexes. The liquid nitrogen X-band ESR spectra of the Fe(I) alkynyls dissolved in THF are generally very complicated and poorly resolved showing both **g** tensor and ^{31}P hyperfine tensor anisotropy.

Fortunately, a spectrum with a much better resolution has been obtained for the heptynyl derivative **11** in 2-methyltetrahydrofuran glass. Indeed, the spectrum (Figure 6, full line) shows a partial resolution of the hyperfine structure due to coupling of the electron spin to the nuclear spin of the phosphorus nuclei of the PP_3 ligand.

A satisfactory computer simulation of the experimental spectrum (Figure 6, dashed line) has been obtained by introducing the following g and A_P values: $g_l = 2.090$ (A_l = 36.0, 20.0, 40.0, and 16.0 G), $g_m = 2.048$ (A_m = 38.0, 20.0, 18.0, and 17.0 G), and $g_h = 1.998$ (A_h = 37.0, 22.5, 18.0, and 17.0 G). Noticeably, the magnetic parameters are consistent with the maintenance of a distorted TBP structure in frozen solution.

Unlike the frozen solution spectra, all fluid solution spectra of the Fe(I)–alkynyl complexes exhibit satisfactory resolution.

A variable-temperature study has provided precious information on the dynamic behavior of the Fe(I) alkynyls in THF solution. The X-band ESR spectra of the heptynyl derivative **11** in THF at 230, 260, and 300 K are shown in Figure 7. At the highest temperature, the spectrum is consistent with the presence of a unique metal species (**A**) in solution. The line shape of the resonance ($\langle g\rangle$ = 2.065) appears as a broad triplet, indicating that the unpaired electron significantly couples ($\langle a_{P_{av}}\rangle$ = 13 G) only to two phosphorus nuclei. In the temperature range from 200 to 230 K, a unique metal species (**B**) is still present which, however, exhibits quite different spectral parameters (doublet of quartets centered at $\langle g\rangle$ = 2.066; $\langle a_P\rangle$ = 18 G, 3P; $\langle a_P\rangle$ = 47 G, 1P). In the temperature range from 230 to 300 K, both species are observed with concentrations that reversibly depend on the temperature (at 260 K species **A** and **B** are in a ca. 3:2 ratio). At temperatures higher than 300 K, the triplet resonance broadens, until at 330 K the spectrum consists of an unresolved singlet.

Identical fluid solution behavior is exhibited by all Fe(I) alkynyls (Table IV).

A reasonable interpretation of the variable-temperature fluid solution spectra may be given in light of previous reports.[7b,c,50] In fact, the overall ESR picture exhibited by the Fe(I) alkynyls closely resembles that of related Rh(II) (d^7 low-spin configuration)

(49) Bencini, A.; Gatteschi, D. *Transition. Met. Chem. (N.Y.)* **1982**, *8*, 1.
(50) (a) Bianchini, C.; Laschi, F.; Ottaviani, M. F.; Peruzzini, M.; Zanello, P.; Zanobini, F. *Organometallics* **1989**, *8*, 893. (b) Bianchini, C.; Peruzzini, M.; Laschi, F.; Zanello, P. *Topics in Physical Organometallic Chemistry*; Gielen, M. F., Ed.; Freund Publishing House Ltd.: London, 1992; Vol. 4.

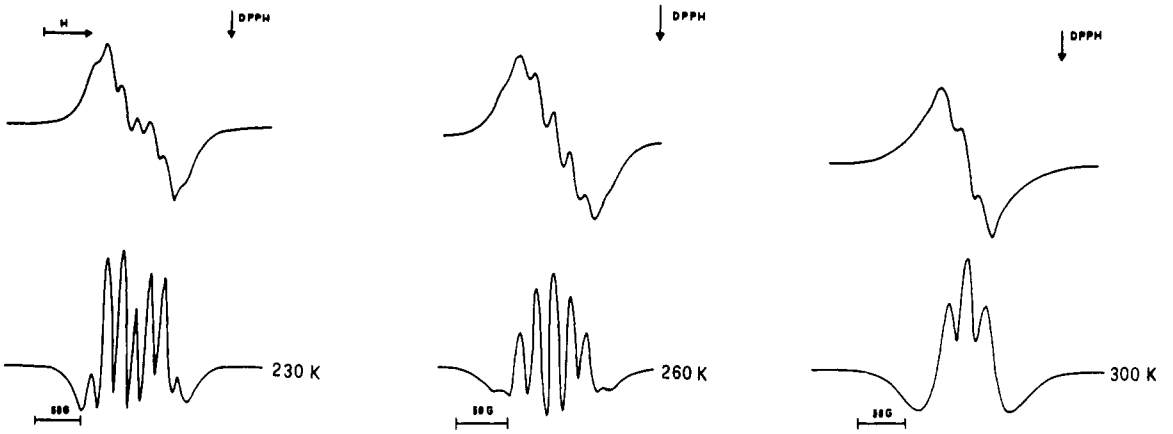

Figure 7. X-band ESR spectra of **11** dissolved in tetrahydrofuran at 230, 260, and 300 K (upper). Second derivative spectra (lower).

complexes of the general formula $[(PP_3)Rh(C{\equiv}CR)]^+$ (R = Ph, CO_2Et, CHO).[7c] In fluid solution, the rhodium compounds exist as two isomeric forms exhibiting distorted square-pyramidal structures in a ratio that reversibly depends on the temperature. A similar situation may well account for the dynamic behavior of the present Fe(I) alkynyls, with the difference that both isomeric iron species would adopt more or less distorted TBP geometries. Actually, one may exclude a temperature-controlled interconversion between trigonal-bipyramidal and square-pyramidal structures of the Fe(I) alkynyls on the basis of the ESR parameters [particularly, the absence of the very large coupling constant of the unpaired electron (200–300 G) to the phosphorus atom of PP_3 which in a square-pyramidal geometry looks at the d_{z^2} SOMO].[7bc,50] On the other hand, the electrochemical data suggest that the addition of one electron to the trigonal-bipyramidal Fe(II) alkynyls causes minor stereochemical rarrangements, a fact that is consistent with the maintenance of the trigonal-bipyramidal structure.

In the absence of actual simulations, however, it is worth mentioning an alternative explanation for the variable-temperature fluid solution spectra exhibited by the Fe(I) alkynyls. The line-shape changes may simply be due to fluxional behavior of the phosphorus donors, similar to what was observed by Ittel et al. for (η^3-cyclooctenyl)$Fe[P(OMe)_3]_3$.[51] In particular, one phosphorus of one kind (47 G) would exchange with any one of three phosphorus nuclei of another kind (18 G). In the slow exchange limit (230 K), the spectrum actually appears as a doublet of quartets, while at high temperature (>300 K) where the exchange is fast on the ESR time scale the phosphorus nuclei would be equivalent (quintet of binomial intensities) by rapid averaging. The fact that the fast exchange spectrum (330 K) consists of an unresolved singlet may be explained by taking into account phosphorus hyperfine couplings of opposite sign [e.g. (3 × 18 − 47)/4 = 1.8 G]. According to this interpretation the spectra in between the slow and fast exchange limits would just be two snapshots at intermediate rates of exchange.

As a concluding remark, it is worth making a comparison with the structure and the ESR spectra of the recently reported Fe(I) complex $[Fe(CO)_3(PPh33)_2]PF_6$.[52] The cation in the latter complex assumes a distorted square-pyramidal structure with trans basal phosphorus (P–Fe–P bond angle of 163.4(1)°, a (basal CO)–Fe–(basal CO) angle of 162.0(6)°). The ESR spectra (doped single crystal) are quite consistent with a $^2A_1$ ground state in C_{2v} symmetry with the unpaired electron principally located in the iron $3d_{z^2}$ orbital. Unlike $[Fe(CO)_3(PPh_3)_2]^+$, the Fe(I) complexes described in this paper maintain, even though largely distorted, the trigonal-bipyramidal structure of the Fe(II) precursors. A reasonable explanation for the different behavior of the PP_3 complexes might be sought in the geometrical constraints of the tripodal ligand in which the donor atoms, being interconnected by alkyl chains, cannot largely move one with respect to the other.[38] However, the PP_3 phosphorus atoms apparently have enough mobility to cause a distortion in the coordination polyhedra of the Fe(I) alkynyls sufficiently large to split the degenerate pair of e levels to such an extent that well-resolved ESR spectra are observable even in room temperature solution.[48,52]

Fe(II) Complexes. All the Fe(II) alkynyls in frozen THF solution display ESR parameters which are in good agreement with those of the powder spectra, indicating that the Fe(II) compounds maintain the TBP geometry in solution (Table V). Minor variations of the magnetic parameters between the powder and solution spectra can be related to the effect of the solvent on the overall line shape.[53] Finally, the absence of ESR signals for the room temperature spectra is attributed to the temperature dependence of the zero-field splitting term in the relevant Hamiltonian $S = 1$ systems.[46–48]

Acknowledgment. This work was supported by the "Progetto Finalizzato Chimica-Fine II, CNR, Rome, Italy. A.P. thanks the Ministerio de Educacion y Ciencia, Spain, for providing a research grant.

Supplementary Material Available: Tables of final positional parameters for all atoms of **1** and **8** (7 pages); listings of observed and calculated structure facrors for **1** and **8** (28 pages). Ordering information is given on any current masthead page.

(51) Ittel, S. D.; Krusic, P. J.; Meakin, P. *J. Am. Chem. Soc.* **1978**, *100*, 3264.

(52) MacNeil, J. H.; Chiverton, A. C.; Fortier, S.; Baird, M. C.; Hynes, R. C.; Williams, A. J.; Preston, K. F.; Ziegler, T. *J. Am. Chem. Soc.* **1991**, *113*, 9834.

(53) Razuva, G.; Cherkasov, V. K.; Abamukov, G. A. *J. Organomet. Chem.* **1978**, *160*, 361.